FY2013 Theory Milestone
First Quarterly Report
December 19, 2012

Submitted by: S. C. Jardin, PPPL jardin@pppl.gov

I. Introduction

We report here on the successful completion of the first quarterly milestone for the FY2013 Theory Target on Disruption Physics as described in the Appendix. This Theory Target is closely related to a Contract between ITER IO and PPPL funded for 3 years starting 15 February 2011. The DOE funded work described here makes possible the ITER funded work described in [1]. The present activity also greatly benefits from the continued development of the massively parallel 3D MHD codes M3D [2] (as well as NIMROD), whose continuing development and optimization is partially funded by the SciDAC Center for Extended Magnetohydrodynamic Modeling (CEMM).

The first quarter milestone (see Appendix) is to redo earlier simulations of VDE's as described in references [3,4] with increased spatial resolution and increased time-scale separation which is enabled by the increased spatial resolution. The increased spatial resolution is in turn enabled by improvements in the parallel scaling of the M3D code and by access to the Hopper computer at NERSC.

The original simulations published in [3] were characterized by 4 parameters as indicated in the "Reference [3]" row in Table 1. The goal of the first quarter milestone is to perform a series of simulations with larger number of radial zones L_D, smaller plasma resistivity η_0, smaller wall resistivity η_W, and similar vacuum resistivity η_V. This will increase the separation of time scales between the resistive diffusion time of the plasma (very long), the resistive decay time of the wall (somewhat shorter), and the resistive time of the intermediate "vacuum" region (very short). This better separation of timescales is needed in order to scale our computational results to ITER parameters.

Table 1: Zoning and dimensionless parameters for original and new simulations.

	Number of radial zones: L_D	Plasma resistivity η_o	Wall resistivity η_W	"Vacuum" resistivity η_V
Ref. [3]	40	10^{-5}	10^{-1}	10^{-2}
Thrust A	60	10^{-6}	10^{-4}	10^{-2}
Thrust B	100	2×10^{-7}	1.5×10^{-3}	10^{-2}
Thrust C	110	5×10^{-6}	5×10^{-2}	6×10^{-2}

For this 1st quarter, we have performed 3 simulations of 3 different tokamaks that each improve the realism of the initial simulations in all parameters. We denote these here as Thrusts A-C. A description of each of these thrusts follows. Thrust A: These simulations are done with a simplified ITER geometry. Thrust B: These simulations are of the ASDEX tokamak, for which experimental data is available. Thrust C: These simulations are of the NSTX tokamak, for which experimental data is available.

II. Thrust A: ITER

We modeled ITER, starting from an eqdsk file provided by the ITER IO, FEAT15MA. We used the M3D-mpp code version, running on hopper.nersc.gov. We allowed the vertical drift of the plasma (VDE) and three dimensional perturbations to evolve simultaneously. As we found in [3], the sideways wall force F_x was a peaked function of $\gamma\tau_{wall}$, where γ is the mode growth rate, and τ_{wall} is the resistive wall penetration time, which is of order of the VDE growth time. In these simulations, the resistivity normalized to the Alfven toroidal transit time τ_A and the device minor radius a was $\eta = 10^{-6}$, and τ_{wall}, normalized in the same way, ranged from $10 < \tau_{wall} < 10^4$. This represents a great improvement over the parameters used in [3]. The peak of $F_x(\gamma\tau_{wall})$ occurred for $\tau_{wall} = 300$. We show a plot of $F_x(\gamma\tau_{wall})$ for these cases. The peak value of F_x was about 15% lower than in [3], but the initial state was somewhat different in those cases. A theory has been developed of the peaking of $F_x(\gamma\tau_{wall})$ and is in good agreement with the numerical results [5].

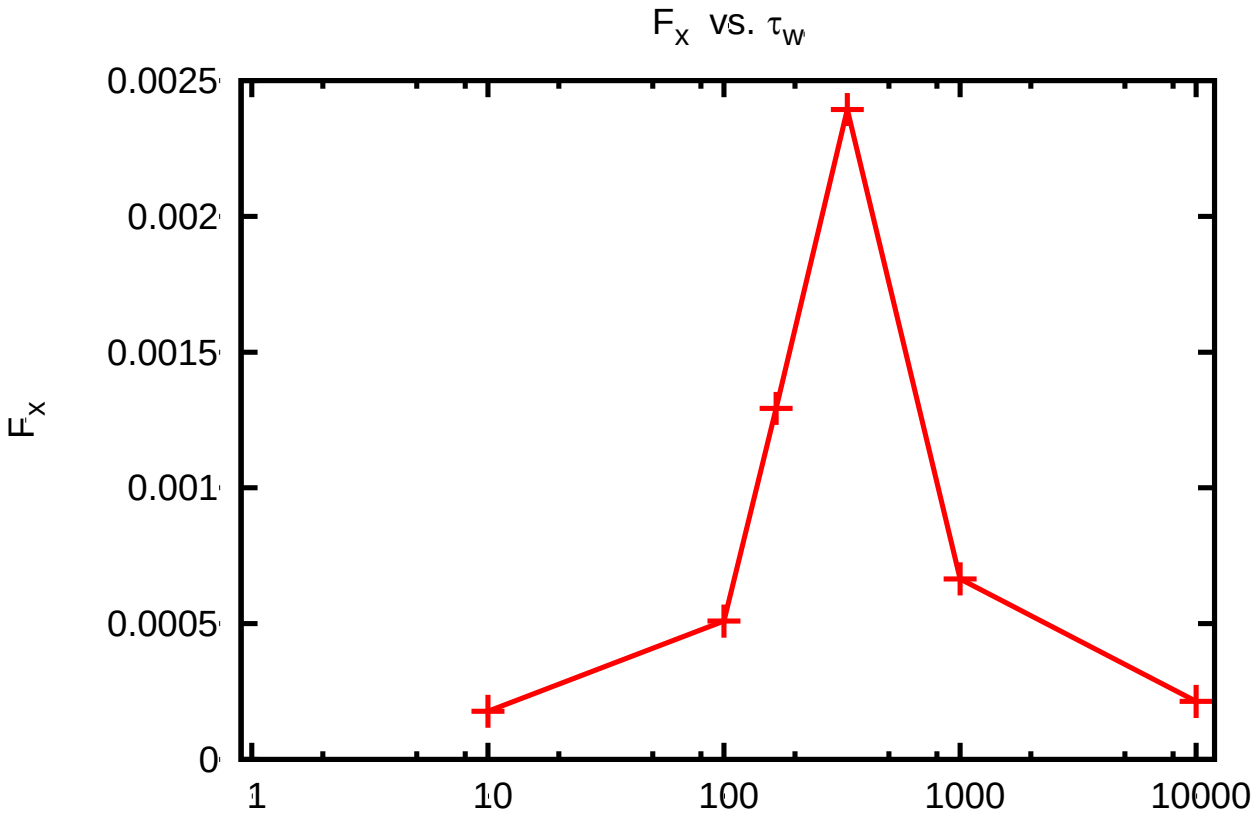

Figure 1: Dependence of the sideways wall force on the dimensionless wall time constant.

III. Thrust B: ASDEX-U

We modeled ASDEX shot #25000 (time label 3.129 s) for which TSC and DINA simulations also exist. We used a resolution of around 30,000 vertices on the poloidal cross section and 16 toroidal planes. The Lunquist number for these simulations was in the range $10^5 \leq S \leq 5\ 10^6$. In the course of performing these simulations we scanned the S values in the whole interval given above and also tested sensitivity to other physical parameters like the plasma viscosity and thermal conductivity. The most important thing that we found is that there is a competition in the system between the VDE time scale (determined by the wall time constant but also influenced by the plasma temperature), the current and temperature evolution in the plasma (determined by the transport and by the Lundquist number) and the evolution of the resistive kink, which determines the final TPF (Toroidal Peacking Factor) (i.e. non axi-symmetry) and halo fraction.

The highest values of the TPF is obtained when the evolution of the VDE and the transport in the plasma is slow enough to permit the kink to grow to a high amplitude before decaying into the wall. An example is shown in Fig.2(a,b), the time evolution of the pressure (poloidal flux contours are also given) during the VDE is shown, for a quasi symmetric case (a) and a non axi-symmetric case (b) (TPF is around 1.3). The Lundquist number is set to $S= 5\ 10^6$ (while the Prandtl number is 500 i.e. viscous dissipation is 500 times higher than resistive dissipation). Both cases are initially perturbed (the initial perturbation is multiplied by a factor 5 in case (b) if compared with (a)).

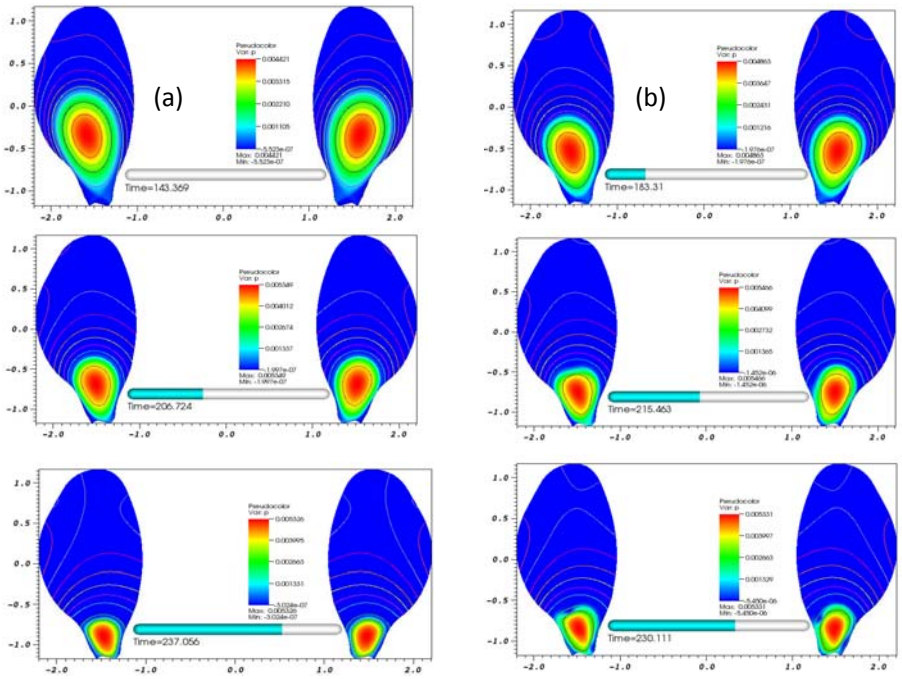

Fig.2(a,b): Pressure and poloidal flux contours in time for a quasi symmetric (a) and a non symmetric (b) VDE.

The halo fraction and the current decay instead (see Fig.3) are similar in the two cases. Note also that the pressure decay traces that of the current.

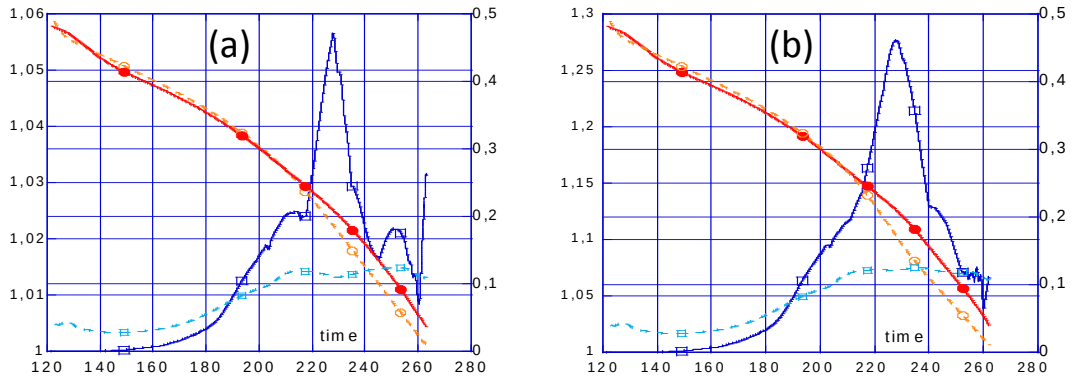

Fig.3:TPF (blue squares, left axis) , current, pressure (red, orange circles) and halo fraction (light blue squares) (right axis) for case (a) and (b) (as in Fig.2). The pressure is multiplied by 250.

We have succeeded running these cases with high resolution and the parameters shown in the table. The main shortcoming of these ASDEX simulations is that the thermal quench occurs much slower than observed in experiments, where it happens much faster than the current quench phase. In our simulations, they happen on approximately the same time scales. The 2D TSC and DINA calculations cause the thermal quench to happen rapidly by artificially increasing the thermal conductivity to a very large value over a very short timescale. We tried to reproduce this phenomena in the 3D calculation from first principles by computing the 3D MHD mode activity and computing parallel transport along open field lines. However, this was not sufficient to reproduce the short timescales of the thermal quench seen in the experiments. We are now refining our MHD model by adding impurity radiation, which is known to be important during the thermal quench. We may need to add other sub-grid-scale models of disruption induced transport to reproduce the experimental times.

VI. Thrust C: NSTX

Our NSTX modeling was based on an equilibrium reconstructed from shot 132859 from XP833, in which the vertical field control system was deliberately switched off mid-shot in order to produce a rapid VDE. The VDE and three-dimensional perturbations evolved simultaneously using the MPI version of the M3D code on a mesh with a resolution of 110 radial zones (about 40,000 vertices/plane) and 12 to 18 toroidal planes. The central plasma resistivity was scanned over two orders of magnitude from 5×10^{-6} to 5×10^{-4}, holding the wall and vacuum resistivities fixed at 5×10^{-2} and 6×10^{-2} respectively. (These relatively large values of wall resistivitities used were to expedite calculations in which the focus was on the plasma and will be lowered future runs.) For the lowest values of plasma resistivity, the kink mode was stable and the VDE remained essentially two-dimensional, producing large transient halo currents and vertical force but with a negligible toroidal peaking factor and horizontal force component. For the highest plasma resistivities, the plasma underwent a kink instability that flattened the temperature profile

before significant vertical displacement had taken place, resulting in relatively low axisymmetric and non-axisymmetric current loads and forces on the vessel. The largest horizontal forces and current peaking factors occurred at an intermediate plasma resistivity for which the kink and vertical instabilities grew on approximately the same time scale, resulting in a strongly helically shaped plasma hitting the wall.

In the following quarters, we plan to repeat these calculations at higher resolution and with a much more realistic wall time by separating the two-dimensional and three-dimensional phases of the instability. This will allow us to make direct comparisons with halo current distribution measurements from the experiment.

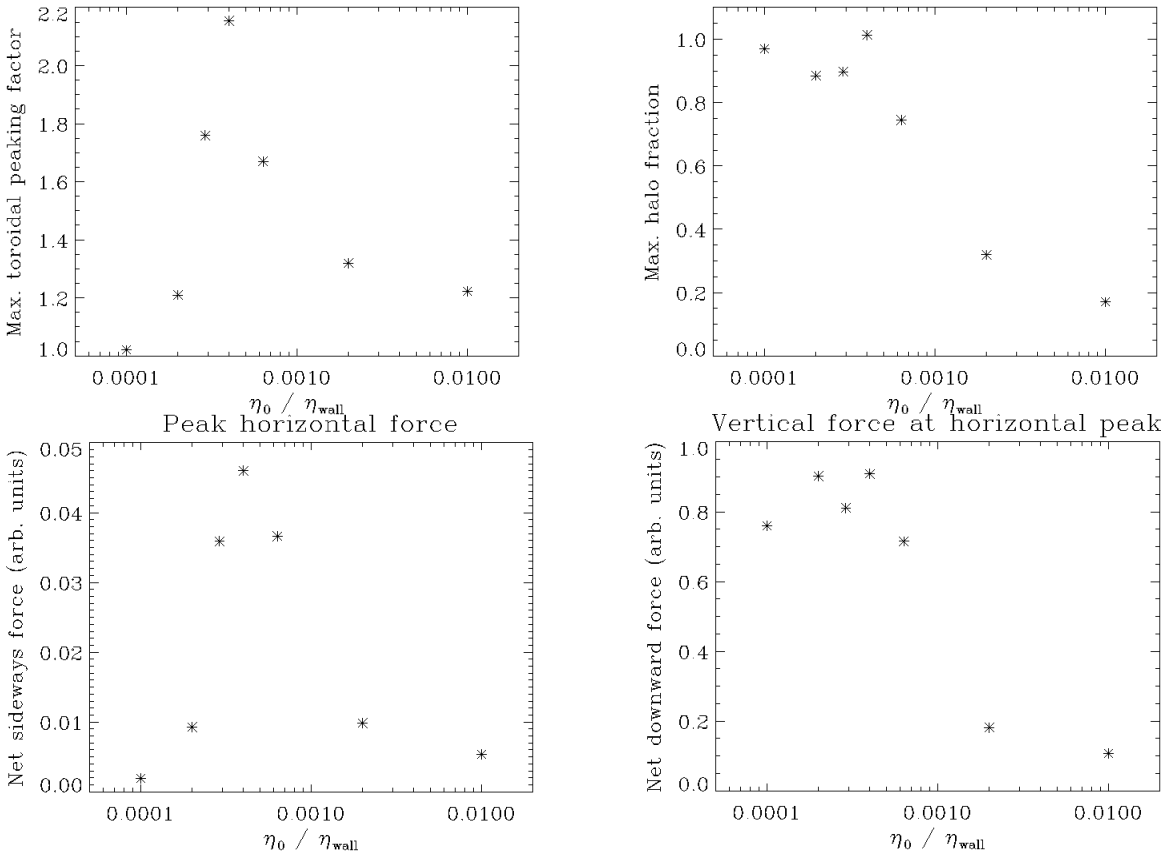

Figure 4: A series of runs with varying plasma resistivity showing the dependence of the resistivity on the maximum toroidal peaking factor (top left), the net sideways force (bottom left), the maximum halo fraction (top right) and the net downward force (bottom right).

V. Summary

During this quarter, we have performed increasingly realistic 3D MHD simulations of 3 tokamaks: ITER, ASDEX, and NSTX. These have provided new insights into the mechanisms by which plasma disruptions can induce large currents and associated large forces into the surrounding vacuum vessel. These results are being used to prepare additional simulations of even greater realism to be reported in the 3rd quarterly report. The present simulations together with the ones in preparation should provide solid scaling data with which to predict the nature and magnitude of the forces expected in ITER.

References:

[1] S. Jardin, *3D MHD simulation of VDEs for detailed evaluation of toroidal peaking factor (TPF) and associated electromagnetic loads*, (2011) PPPL Proposal in response to ITER Call for Proposals.

[2] W. Park, E. V. Belova, G.Y. Fu, X. Tang, H. R. Strauss, L. Sugiyama, *Simuation studies using multilevel physics models,* Phys. Plasmas **6**, 1796 (1999)

[3] Strauss, H.R., Paccagnella, R., Breslau, J., *Wall forces produced during ITER disruptions*, Physics of Plasmas (2010) **10** 082505

[4] Paccagnella, R, Strauss, H.R. Breslau, J, *3D MHD VDE and disruptions simulations of tokamak plasmas including some ITER scenarios,* Nuclear Fusion (2009) **49** 035003

[5] H. Strauss, R. Paccagnella, J. Breslau, L. Sugiyama, S. Jardin and R. Sayer, *Sideways wall force produced during disruptions,* paper TH/P3-01, IAEA FEC Conference, 2012. (submitted to Nuclear Fusion)

Appendix: FY 2013 Theory Target on Disruption Physics:

Carry out advanced simulations to address two of the most problematic consequences of major disruptions in tokamaks: the generation and subsequent loss of high-energy electrons (runaway electrons), which can damage the first wall, and the generation of large electromagnetic loads induced by disruptions, and assess the severity of these effects on ITER

Quarterly Milestones:

Q1. Perform a 3D MHD simulation of a vertical displacement event (VDE) disruption at twice the resolution and wall time constant of previous studies to determine the scaling of the 3D forces on the axisymmetric conducting structures, and how these forces differ from those obtained in 2D calculations.

Q2. Perform a 3D MHD simulation of a DIII-D mitigated disruption experiment with symmetric impurity source terms to determine the effects of the source terms and MHD activity on test-particle runaway electron confinement.

Q3. Extend the 3D MHD simulations of VDEs to higher resolution by again doubling the grid resolution and increasing the simulation time period from that used in Q1. This will allow an increase in the Lundquist number to $S=10^6$ and a further doubling of the wall time-constant.

Q4. Extend the simulations of the DIII-D mitigated disruptions to model the effect of spatially non-symmetric source terms on runaway electron confinement.